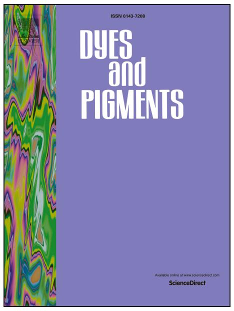

Tunable crystal packing for enhanced electroluminescent properties based on novel thiazole derivatives with different connecting positions of carbazole

Yongqi Bai, Bingwu Wei, Xinhua Ouyang, Zhiyang Liu, Weigang Jiang, Wang Li, Lei Zhang, Ling Hong, Gufeng He, Yali Chen, Ziyi Ge

PII: S0143-7208(16)30091-2

DOI: 10.1016/j.dyepig.2016.03.031

Reference: DYPI 5156

To appear in: *Dyes and Pigments*

Received Date: 15 January 2016

Revised Date: 16 March 2016

Accepted Date: 17 March 2016

Please cite this article as: Bai Y, Wei B, Ouyang X, Liu Z, Jiang W, Li W, Zhang L, Hong L, He G, Chen Y, Ge Z, Tunable crystal packing for enhanced electroluminescent properties based on novel thiazole derivatives with different connecting positions of carbazole, *Dyes and Pigments* (2016), doi: 10.1016/j.dyepig.2016.03.031.

Tunable crystal packing for enhanced electroluminescent properties based on novel thiazole derivatives with different connecting positions of carbazole

Yongqi Bai,[1,2] Bingwu Wei,[3] Xinhua Ouyang,[2] Zhiyang Liu,[2] Weigang Jiang,[2] Wang Li,[2] Lei Zhang,[2] Ling Hong,[2] Gufeng He*[3],Yali Chen,[1]* Ziyi Ge[2]*

[1]*Department of Chemistry, Innovative Drug Research Center, Shanghai University, Shanghai 200444, China*

[2]*Ningbo Institute of Materials Technology and Engineering, Chinese Academy of Sciences, Ningbo 315201, P. R. China*

[3]*National Engineering Lab for TFT-LCD Materials and Technologies, and Department of Electronic Engineering, Shanghai Jiao Tong University, Shanghai 200240, People's Republic of China*

Corresponding Authors: geziyi@nimte.ac.cn; ylchen@staff.shu.edu.cn; gufenghe@sjtu.edu.cn

Abstract Two novel deep-blue fluorescent compounds, namely, 2-(4-(9-phenyl-9H-carbazol-3-yl)phenyl)benzo[d]thiazole (BCzBTZ) and 2-(4'-(9H-carbazol-9-yl)-[1,1'-biphenyl]-4-yl)benzo[d]thiazole (CzBBTZ) were designed, synthesized and characterized. It is particularly intriguing to compare their crystal packing of BCzBTZ and CzBBTZ, both of them construct with the same heterocyclic units and linker. Their crystal packing can be effectively regulated by changing the connecting position of carbazole. Their thermal stabilities, optical and electrochemical properties were studied systematically and exhibited ideal performance for electroluminescent emitters. The device based on BCzBTZ as emitter shows deep-blue emission with the CIE(x, y) of (0.15, 0.08), which is close to the blue standard (0.14, 0.08) of National Television System Committee (NTSC). The maximal external quantum efficiency is 1.4 % and current efficiency is 1.39 cd/A with low efficiency roll-off.

Keywords Thiazole derivatives; Electroluminescence; Tunable crystal packing

Introduction

Heterocyclic compounds have been attracting extensive research interest for organic light-emitting diodes (OLEDs), organic solar cells (OSCs), and organic field-effect transistors (OFETs) due to their semiconducting features [1-2]. For OLEDs, the balance of carries play an important role to achieve high device performance [3]. To solve this issue, some effective strategies have been demonstrated including the fabrication of multilayer devices and development of novel bipolar molecules [4-6]. Regarding the promising potential of bipolar structures for low-cost OLEDs, it is highly desirable to design and synthesize novel multifunctional materials with different heterocyclic units.

In the past decades, numerous multifunctional materials have been developed and some of them show excellent performance, including triarylamine-imidazole, triarylboron-bis(diphenylamino)carbazole, phenoxazine-quinoline, carbazole-1,3,4-diaryloxadiazole, triarylamine-1,3,4-diaryloxadiazole, and so on, especially for the derivatives of triarylamine-imidazole with hybridized local and charge-transfer characteristics [7-14]. By scanning these heterocyclic structures, thiazole, a well-known molecule in the azole family by replacing a carbon with nitrogen atom of thiophene, has been studied and exhibit modest electron-deficient properties, indicating a good candidate for constructing functional emitters. However, to the best of our knowledge, the research on thiazole and its derivatives for electroluminescence is still limited [15]. On the other hand, molecular packing in film or solid state greatly affects their charge transport properties and fluorescent quantum yield. Generally, the transport of carries is mainly depended on their electronic couplings and the reorganization energies [16]. The electronic coupling is strongly based on their molecular packing modes [17]. Therefore, tunable molecular packing or crystal packing are desired to obtain effective electroluminescent materials.

Herein, a couple of benzothiazole derivatives, 2-(4-(9-phenyl-9H-carbazol-3-yl)-phenyl)benzo[d]thiazole (BCzBTZ) and 2-(4'-(9H-carbazol-9-yl)-[1,1'-biphenyl]-4-yl)benzo[d]thiazole (CzBBTZ), was designed and synthesized with a strong electron-donating carbzole (Cz) and electron-accepting thiazole units as shown in Scheme 1. Both of them construct with the same heterocyclic units and linker and only the connecting position of Cz is changed. It is particularly intriguing to compare their crystal packing of BCzBTZ and CzBBTZ. Their crystal packing modes are effectively regulated. The thermal stabilities, optical and electrochemical properties were studied systematically and exhibited ideal performance for electroluminescence emitters. The electroluminescent device based on BCzBTZ as emitter shows deep-blue emission with the CIE(x, y) of (0.15, 0.08), which is close to the blue standard (0.14, 0.08) of NTSC. The maximal external quantum efficiency is 1.4 % and current efficiency is 1.39 cd/A. Furthermore, at the high luminescence, the device still indicated good performance with relatively low efficiency roll-off.

2. Experimental

2.1 Chemicals and instruments

The reagents and starting materials, including 2-(4-bromophenyl)benzo[d]thiazole, bis(pinacolato)diboron, 3-bromo-9-phenyl-9H-carbazole and 9-(4-bromophenyl)-9H-carbazole, were purchased from local suppliers or TCI and used without further purification. ^{1}H NMR spectra was measured on a Bruker DRX-400 spectrometer. Thermogravimetric analysis (TGA) were performed on a TA Q500 instrument. Their optical properties (UV-Vis and fluorescent emission) were done on a Shimadzu UV-2550 and Shimadzu RF-5301PC spectrophotometers. Cyclic voltammetry (CV) measurements were performed on a CHI 660D electrochemical workstation using a Pt wire as the counter electrode, glass-carbon as the working electrode, and a Hg/HgCl electrode as the reference electrode in a dichloromethane solution containing 0.1 M of tetrabutylammonium hexafluorophosphate as the supporting electrolyte. Single-crystal XRD data was collected on Bruker SMART 1000 CCD diffractometer collection. The empirical absorption correction was applied by using the SADABS program [18]. Single crystals of them were solved using direct method, and refined by full-matrix least-squares on F^2 [19].

2.2 Synthesis

2.2.1 *Synthesis of 2-(4-(4,4,5,5-tetramethyl-1,3,2-dioxaborolan-2-yl)phenyl)benzo[d]-thiazole*

A mixture of 2-(4-bromophenyl)benzo[d]thiazole (5.80 g, 20 mmol), bis(pinacolato)diboron (7.62 g, 30 mmol), $PdCl_2$(dppf) (150 mg, 0.2 mmol) and KOAc (8.00 g, 81 mmol) suspended in 70 mL of 1,4-dioxane under the protection of argon was stirred at 87 ^oC for 4 h. After cooling, the mixture was forced through a short pad of silica with dichloromethane (DCM). The solvent was removed under reduced pressure and the crude product was absorbed onto silica. Chromatography on silica gel with gradient elution and a white solid was got (6.40 g, yield: 95%). ^1H NMR (400 MHz, $CDCl_3$) δ [ppm] 8.05-8.10 (m, 3H), 7.87-7.95 (m, 3H), 7.48 (t, 1H, J=7.54Hz), 7.37 (t, 1H, J=7.40Hz), 1.24 (s, 12H).

2.2.2 *Synthesis of 2-(4-(9-phenyl-9H-carbazol-3-yl)phenyl)benzo[d]thiazole (BCzBTZ)*

2-(4-(4,4,5,5-tetramethyl-1,3,2-dioxaborolan-2-yl)phenyl)benzo[d]thiazole (1.69 g, 5 mmol), 3-bromo-9-phenyl-9H-carbazole (1.61 g, 5 mmol) and $PdCl_2(PPh_3)_2$ (100 mg, 0.14 mmol) were added to a 250 ml flask with 40 mL toluene, 20 mL 2M K_2CO_3 and 20 mL ethanol. The mixture was heated to 100 ^oC and stirred for 24 h. After cooling, the mixture was extracted with DCM, organic layer was collected and dried with $MgSO_4$. The solvent was removed and purified by chromatography on silica gel with gradient elution. 1.63g white solid was obtained with yield of 72%. ^1H NMR (400 MHz, $CDCl_3$) δ[ppm] 8.43 (s, 1H), 8.20-8.24 (m, 3H), 8.11 (d, 1H, *J*=8.24 Hz), 7.93

(d, 1H, *J*=7.95 Hz), 7.86 (d, 2H, *J*=8.30 Hz), 7.72 (d, 1H, *J*=8.67 Hz), 7.57-7.66 (m, 4H), 7.44-7.54 (m, 3H), 7.37-7.45 (m, 3H), 7.30-7.35 (m, 1H). ^{13}C NMR (400 MHz, $CDCl_3$) δ 168.1, 154.0, 144.7, 141.4, 140.8, 137.5, 134.9, 132.1, 131.5, 130.0, 128.1, 127.7, 127.6, 127.1, 126.4, 126.3, 125.3, 125.2, 124.0, 123.4, 123.1, 121.6, 120.4, 120.3, 118.9, 110.2, 110.0. Anal. Calcd for $C_{31}H_{20}N_2S$: C, 82.27; H, 4.45; N, 6.19; S, 7.09; Found: C, 82.20; H, 4.49; N, 6.25; S, 7.06. ESI-MS (m/z): 452.99 (M^+). FTIR (KBr, cm^{-1}) 3039 (C-H), 1625 (C=N) ,1596, 1502, 1473, 1453 (C=C), 1233 (C-N), 965 (C-S).

2.2.3 Synthesis of 2-(4'-(9H-carbazol-9-yl)-[1,1'-biphenyl]-4-yl)benzo[d]thiazole (CzBBTZ)

The synthesis of CzBBTZ is carried out in the same procedure as BCzBTZ. Yied=75%. ^{1}H NMR (400 MHz, $CDCl_3$) δ [ppm] 8.24-8.28 (m, 2H), 8.20 (d, 2H, *J*=7.79Hz), 8.15 (d, 1H, *J*=7.99Hz), 7.97 (d, 1H, *J*=7.84Hz), 7.89-7.73 (m, 2H), 7.83-7.87 (m, 2H), 7.69-7.73 (m, 2H), 7.41-7.58(m, 6H), 7.32-7.37(m, 2H). ^{13}C NMR (400 MHz, $CDCl_3$) δ 167.6, 154.1, 142.8, 140.8, 139.0, 137.6, 135.0, 132.8, 128.5, 128.2, 127.6, 127.4, 126.5, 126.0, 125.3, 123.5, 123.2, 121.7, 120.4, 120.1, 109.8. Anal. Calcd for $C_{31}H_{20}N_2S$: C, 82.27; H, 4.45; N, 6.19; S, 7.09; Found: C, 82.17; H, 4.40; N, 6.24; S, 7.19. ESI-MS (m/z): 453.01 (M^+). FTIR (KBr, cm^{-1}) 3041 (C-H), 1622 (C=N), 1595, 1508, 1479, 1450 (C=C), 965 (C-S).

2.3. Device fabrication and characterization

Before the fabrication of devices, BCzBTZ and CzBBTZ were further purified by sublimation. The ITO-coated glass substrates were thoroughly cleaned in an ultrasonic bath using detergent, deionized water, acetone and isopropyl alcohol in turn and then treated with UV-ozone for 15 min. The device was constructed with the structure of MoO_3 (3 nm)/NPB (50 nm)/emission layer (30 nm)/TPBI (30 nm)/LiF/Al. The deposition rate of organic compounds was 0.9-1.1 Å s^{-1}. The electroluminescence spectra and the Commission Internationale de l'Eclairage coordination of the device were tested on a PR655 spectra scan spectrometer. The luminance-current and density-voltage characteristics were measured simultaneously from the measurement of the EL spectra by combining the spectrometer with a Keithley 2400 programmable voltage-current source.

3. Results and discussion

3.1 Synthesis and crystal structures

The synthetic routes of BCzBTZ and CzBBTZ were shown in Scheme 1. Both of them were prepared through one step of Suzuki coupling with 2-(4-(4,4,5,5-tetramethyl-1,3,2-dioxaborolan-2-yl)phenyl)benzo[d]-thiazole and 9-(4-bromophenyl)-9H-carbazole/3-bromo-9-phenyl-9H-carbazole. The important intermediate of 2-(4- (4,4,5,5-tetramethyl-1,3,2-dioxaborolan-2-yl)phenyl)benzo[d]-thiazole was synthesized by Suzuki-Miyaura reaction with 2-(4-bromophenyl)benzo[d]thiazole and 4,4,4',4',5,5,5',5'-octamethyl-2,2'-bi(1,3,2-dioxaborolane). The target compounds were identified by NMR and Single crystal XRD.

Single crystals of BCzBTZ and CzBBTZ were obtained by the slow solvent vapor diffusion method [20]. The detailed crystallographic data are summarized in Tables 1. The single crystals with dimensions of 0.25 mm × 0.14 mm × 0.02 mm for BCzBTZ and 0.30 mm × 0.17 mm × 0.03 mm for CzBBTZ were mounted on a Smart 1000 CCD diffractometer using a graphite-monochromatic Cu-Kα radiation at 296K and 293K, respectively. As shown in Figure 1, both of the crystals belonged to monoclinic system and were asymmetric. Figure 1(b) shows the stacking structure with all atoms along the Axis b for BCzBTZ and the Axis c for CzBBTZ. An intermolecular hydrogen bond between the N atom and the H atom in the crystal package of BCzBTZ is observed. The stacking structures omitting hydrogen atoms for clarity were shown in Figure 1(d).

As well-known, the better planarity for a molecule means a better π-electronic conjugation and it is very important for OLED materials. However, a large plane will quench their fluorescence in the film. Therefore, it is very important to choose a balance both of them. From the Figure 1(d), a small twisted angle is found between the carbazole unit and the benzene ring in BCzBTZ, while the benzene ring and benzothiazole block are almost on a plane, which is contributed to intramolecular electron-transfer and hole-transfer [21]. In crystal package of BCzBTZ, the plane of the two adjacent molecules exhibits a good parallelism and means a better conjugation of π-electronic cloud between them, that is beneficial to the transfer of carries between molecules in the film. For CzBBTZ, although the benzene ring and benzothiazole units have a good planarity, while the carbazole is almost perpendicular to the benzene ring, which means the carries can not transport fluently between carbazole and benzothiazole. In crystal package of CzBBTZ, the plane of the two adjacent molecules is almost vertical and it will affect the carrier transfer in the devices.

3.2 Thermal and electrochemical properties

The thermal properties of BCzBTZ and CzBBTZ were measured by TGA under a nitrogen atmosphere. Results are shown in Table 2 and Figure 2(a). Their decomposition temperatures (T_d, corresponding to 5% weight loss) are found to be 340 and 347 °C for CzBBTZ and BCzBTZ, respectively. Such T_d values indicate that both of them are stable and have the potential to be fabricated into devices by vacuum thermal evaporation technology. The energy levels of them are calculated according to the measurement of cyclic voltammetry (Figure 2(b)) and film absorption (Figure 3(a)). As shown in Figure 2(b), the oxidation onset potentials of them are 0.91 eV for BCzBTZ and 0.92 eV for CzBBTZ, the corresponding highest occupied molecular orbital (HOMO) levels can be estimated to be -5.71 eV for BCzBTZ and -5.70 eV for CzBBTZ, respectively, by comparing with ferrocene (Fc) ($\mathrm{HOMO} = -(E_{ox} + 4.8)$ eV) [22]. Apparently, the HOMO levels are elevated significantly compared to that of TPBI (HOMO level of -6.2 eV), implying an enhanced hole injection ability [23]. By combining the values of energy gaps from film absorption, their lowest unoccupied molecular orbital (LUMO) energy levels are -2.73 eV for BCzBTZ and -2.65 eV for CzBBTZ. Likewise, their LUMO levels are close to that of TPBI (LUMO level of -2.7 eV), showing suitable electron injection ability.

3.3 Absorption and photoluminescent properties

The ultraviolet-visible (UV-vis) absorption and photoluminescent (PL) properties of BCzBTZ and CzBBTZ in dilute DCM solution as well as film are studied as shown in Figure 3 and Table 1. As illustrated in Figure 3(a), both of them show similar absorption profiles with two peaks at ~340 nm and ~300 nm in the dilute solution, which is assigned to the internal charge transfer (ICT) transition and the $\pi-\pi^*$ transition, respectively [24]. For the absorption of neat films, their maximal absorption is red-shifted in relation to the solution measurements due to the H-type molecular aggregation [25]. According to the absorption edges of films, optical energy band gaps (E_g^{opt}) of BCzBTZ and CzBBTZ are 2.98 and 3.07 eV, respectively. Their fluorescence properties were studied by measuring their PL spectra in both DCM solution and solid-state thin films on quartz substrates. As seen in Figure 3(b), they exhibit a deep-blue emission with the maximal wavelength of 448 nm for BCzBTZ and 452 nm for CzBBTZ. It should be noted that BCzBTZ show negligibly small peak shifts in their PL spectra from dichloromethane solutions to solid states. This indicates that the highly twisted structure between the thiazole and Cz units as well as the noncoplanar N-phenylcarbazole moiety can effectively suppress the intermolecular $\pi-\pi$ stacking in the solid state. In addition, the PL spectrum of BCzBTZ and CzBBTZ shows obvious solvatochromic shift, in which their emission color is red-shifted with increasing solvent polarity (Figure 3 (c) and (d)). This indicates the occurrence of charge transfer upon photoexcitation.

3.4 Theoretical calculations

In order to understand the electronic structures, their molecular configurations and orbital distributions were predicated by using Gaussian software with density functional theory (DFT) method at the B3LYP/6-31G(d,p) level. As shown in Figure 4, the HOMO level mainly locates on the Cz part for CzBBTZ, while BCzBTZ shows on the whole molecule. In other words, the Cz moiety contributes less to the HOMO energy in BCzBTZ compared with that of CzBBTZ. The calculated HOMO levels of them are -5.31 eV and -5.37 eV, respectively. The LUMO levels mostly locate on the benzothiazole ring and their linkers between donor and acceptor. It is noted that the large overlap of LUMO and HOMO in BCzBTZ would be beneficial for the charge transfer as the emitter in OLED. On the other hand, it could facilitate the charge transfer process upon excitation, which was also confirmed by the solvatochromic phenomenon observed in the solvents with a different polarity.

3.5 Electroluminescent properties

To investigate their electroluminescent performance, non-dopant fluorescence OLEDs with the following configuration: ITO/MoO_3 (3 nm)/NPB (50 nm)/BCzBTZ or CzBBTZ (30 nm)/TPBI (30 nm)/LiF (1 nm)/Al was fabricated, where MoO_3 and LiF were utilized as a hole-injection layer and an electron-injection layer, respectively; NPB acted as a hole-transporting layer; TPBI was used as the electron-transporting and the hole-blocking layer. The energy levels of the used materials were shown in

Figure 5. Their current density–voltage (*J*–*V*) characteristics, voltage–luminescence (*V*–*L*) profiles, current efficiencies-current density, and electroluminescent spectra for the devices were plotted in the Figure 6 and some key paramaters were summarized in Table 3.

Figure 6 (a) shows the current density-voltage (*J*-V) curves of BCzBTZ or CzBBTZ. The turn-on voltage of the device with BCzBTZ is 3.2 V at the luminance of 1 cd m^{-2}, while the device with CzBBTZ is up to 5.5 V, which is about twice higher than that of BCzBTZ-based device. It means that the charges injection is easy in the device with BCzBTZ as emitter. The voltage-luminance results are shown in Figure 6 (b). Obviously, the maximum luminance brightness of BCzBTZ is 8295 cd m^{-2} at 9 V, while the corresponding CzBBTZ exhibits only 812 cd m^{-2}. The brightness of BCzBTZ-based device is more than 10 times higher than those obtained from the CzBBTZ-based device, which can be attributed to the low fluorescent quantum yield and difficult charges injection. As shown in Figure 6 (c), the maximum current efficiency for BCzBTZ is 1.39 cd A^{-1}, and external quantum efficiency (EQE) is 1.4%. CzBBTZ exhibited a low performance with the maximum current efficiency of 0.52 cd A^{-1}, and external quantum efficiency (EQE) of 0.2%, respectively. It is notable that the devices with BCzBTZ as emitter exhibits a low efficiency roll-off at high current density.

The maximum EL emission $\lambda_{\max}$ of BCzBTZ and CzBBTZ is located at 440 nm and the FWHM value is 50 and 60 nm, respectively. Compared with PL, there is a 10 nm blue-shift for the emission peak in EL spectrum. The blue-shift can be ascribed to the face-to-face π-π stacking in the vacuum-deposited film [26]. When the current density is at the brightness of 100 cd/m^2, the CIE coordinates (x, y) of BCzBTZ device is found to be (0.15, 0.08), which is close to the pure blue standard (0.14, 0.08) of NTSC.

4. Conclusions

In summary, we demonstrated two novel deep-blue fluorescent compounds with thiazole as electron-transporting and carbazole as hole-transporting blocks for electroluminescent emitters. Their thermal stabilities, optical and electrochemical properties were studied systematically and exhibited ideal performance for OLED emitters. Interestingly, their crystal packing can be effectively regulated by changing the connecting position of carbazole. The device based on BCzBTZ as emitter shows pure deep-blue emission with the CIE (x, y) of (0.15, 0.08) and good performance with maximal external quantum efficiency of 1.4 % and current efficiency of 1.39 cd/A, implying that thiazole has potential application in the design of new fluorescent molecules for OLEDs.

Acknowledgements This work was financially supported from National Natural Science Foundation of China (21574144, 51273209, 51411140244), CAS Interdisciplinary Innovation Team, Zhejiang Provincial Natural Science Foundation of China (LR16B040002), and Ningbo Municipal Science and Technology Innovative Research Team (2015B11002).

References

[1] Zhuang J, Li. W, Su W, Zhou M, Cui Z. Novel ternary bipolar host material with carbazole, triazole and phosphine oxide moieties for high efficiency sky-blue OLEDs. New J Chem 2014; 38: 650-6.

[2] Ye L, Jiao X, Zhou M, Zhang S, Yao H, Zhao W, et al. Manipulating Aggregation and Molecular Orientation in All-Polymer Photovoltaic Cells. Adv Mater 2015; 27: 6046-54.

[3] Ouyang X, Zeng H, Ding G, Jiang W, Li J. Luminance materials containing carbazole and triphenylamine exhibiting high hole-transporting properties. Synthetic Met 2009; 159: 2063-9.

[4] Liu M, Li X, Chen D, Xie Z, Cai X, Xie G, et al. Study of configuration differentia and highly efficient, deep-blue, organic light-emitting diodes based on novel naphtho[1,2- d]imidazole derivatives. Adv Funct Mater 2015; 25: 5190-8.

[5] Prachumrak N, Pojanasopa S, Tarsang R, Namuangruk S, Jungsuttiwong S, Keawin T, et al. Synthesis and characterization of carbazole dendronized coumarin derivatives as solution-processed non-doped emitters and hole-transporters for electroluminescent devices. New J Chem 2014; 38: 3282-94.

[6] Ge Z, Hayakawa T, Ando S, Ueda M, Akiike T, Miyamoto H, et al. Spin-coated highly efficient phosphorescent organic light-emitting diodes based on bipolar triphenylamine-benzimidazole derivatives. Adv Funct Mater 2008; 18: 584-90.

[7] Li W, Liu D, Shen F, Ma D, Wang Z, Feng T, et al. A twisting donor-acceptor

molecule with an intercrossed excited state for highly efficient, deep-blue electroluminescence. Adv Funct Mater 2012; 22: 2797-803.

[8] Ouyang X, Li X, Ai L, Mi D, Ge Z, Su S. Novel “hot exciton” blue fluorophores for high performance fluorescent/phosphorescent hybrid white organic light-emitting diodes with superhigh phosphorescent dopant concentration and improved efficiency roll-off. ACS Appl Mat Interfaces 2015; **7**: 7869-77.

[9] Ouyang X, Li X, Bai Y, Mi D, Ge Z, Su S. Highly-efficient hybrid white organic light-emitting diodes based on a high radiative exciton ratio deepblue emitter with improved concentration of phosphorescent dopant. RSC Adv 2015; 5: 32298-306.

[10] Suzuki K, Kubo S, Shizu K, Fukushima T, Wakamiya A, Murata Y, et al. Triarylboron-based fluorescent organic light-emitting diodes with external quantum efficiencies exceeding 20%. Angew Chem Int Ed 2015; 54: 15231-5.

[11] Kulkarni AP, Zhu Y, Babel A, Wu P, Jenekhe S. New ambipolar organic semiconductors. 2. Effects of electron acceptor strength on intramolecular charge transfer photophysics, highly efficient electroluminescence, and field-effect charge transport of phenoxazine-based donor-acceptor materials. Chem Mater 2008; 20: 4212-23.

[12] Gong S, Chen Y, Zhang X, Cai P, Zhong C, Ma D, et al. High-performance blue and green electrophosphorescence achieved by using carbazole-containing bipolar tetraarylsilanes as host materials. J Mater Chem 2011; 21: 11197-204.

[13] Dumur F, Goubard F. Triphenylamines and 1,3,4-oxadiazoles: a versatile combination for controlling the charge balance in organic electronics. New J. Chem

2014; 38: 2204-24.

[14] Li W, Pan Y, Yao L, Liu H, Zhang S, Wang C, et al. A hybridized local and charge-transfer excited state for highly efficient fluorescent OLEDs: molecular design, spectral character, and full exciton utilization. Adv Optical Mater 2014; 2: 892-901.

[15] Xiao G, Lei P, Chi H, Lu Y, Dong Y, Hua Z, et al. Synthesis and luminescence of red, fluorinated iridium (III) complexes containing alkenyl benzothiazole ligand. Synthetic Met 2009; 159: 705-9.

[16] Bin Z, Duan L, Qiu Y. Air dtable organic dalt ss an n−type fopant for efficient and stable organic light-emitting diodes. ACS Appl Mater Interfaces 2015; **7**: 6444-50.

[17] Dou J, Zheng Y, Yao Z, Yu Z, Lei T, Shen X, et al. Fine-tuning of crystal packing and charge transport properties of BDOPV derivatives through fluorine substitution. J Am Chem Soc 2015; 137: 15947-56.

[18] Krause L, Herbst-Irmer R, Stalke D. An empirical correction for the influence of low-energy contamination. J Appl Crystallogr 2015; 48: 1907-13.

[19] Murugavel S, Lakshmanan D, Nagarajan S, Ponnuswamy A. Synthesis and crystal structure of 6-(1-benzyl-5-methyl-1H-1,2,3-triazol-4-yl)-4-(2-methoxyphenyl)-3,4-dihydropyrimidine-2(1H)-thione. Bulg Chem Commun 2015; 47: 50-4.

[20] Zang L, Che Y, Moore J. One-dimensional self-assembly of planar π-conjugated molecules: adaptable building blocks for organic nanodevices. Acc Chem Res 2008; 41: 1596-608.

[21] Ramirez C, Procaccine R, Chesta C, Parest A, Vera D. Selective charge transfer in donor/acceptor systems bridged by Tröger base derivatives. Org Electron 2013;14: 2564-72.

[22] Ouyang X, Peng R, Ai L, Zhang X, Ge Z. Efficient polymer solar cells employing a non-conjugated small-molecule electrolyte. Nat. Photonics 2015; 9: 520-5.

[23] Wang Z, Liu C, Zheng C, Wang W, Xu C, Zhu M, et al. Efficient violet non-doped organic light-emitting device based on a pyrene derivative with novel molecular structure. Org Electron 2015, 23, 179-85.

[24] Chen L, Jiang Y, Nie H, Hu R, Kwok H, Huang F, et al. Rational design of aggregation-induced emission luminogen with weak electron donor-acceptor interaction to achieve highly efficient undoped bilayer OLEDs. ACS Appl Mater Interfaces 2014; 6: 17215-25.

[25] Ouyang X, Wang G, Zeng H, Zhang W, Li J. Design and synthesis of 2-substituted-8-hydroxyquinline zinc complexes with hole-transporting ability for highly effective yellow-light emitters. J Organomet Chem 2009; 694: 3511-7.

[26] Wang Z, Feng Y, Li H, Gao Z, Zhang X, Lu P, et al. Dimeric phenanthro-imidazole for blue electroluminescent materials: the effect of substituted position attached to biphenyl center. Phys Chem Chem Phys 2014; 16: 10837-43.

Tables

Table 1 Crystallographic data and structure refinement parameters of BCzBTZ and CzBBTZ

Table 2 The physical parameters of the compounds BCzBTZ and CzBBTZ

Table 3 Electroluminescent characteristics of the devices with the structure of ITO/MoO_3 (3 nm)/NPB (50 nm)/BCzBTZ or CzBBTZ (30 nm)/TPBI (30 nm)/LiF (1 nm)/Al.

Table 1.

Compound	BCzBTZ	CzBBTZ
Empirical formula	$C_{30}H_{20}N_2S$	$C_{30}H_{20}N_2S$
Formula weight	452.55	452.55
Temperature (K)	296(2)	293(2)
Crystal system	Monoclinic	Monoclinic
Space group	P2(1)/n	P2(1)/n
a (Å)	15.88(5)	8.1907(18)
b (Å)	7.82(2)	34.463(7)
c (Å)	17.46(5)	8.3321(18)
α (°)	90	90
β (°)	92.54(4)	103.940(3)
γ (°)	90	90
V (Å^3)	2165(11)	2282.7(8)
Z	4	4
D_c (Mg/m^3)	1.388	1.317
μ (mm^{-1})	0.174	0.165
F(000)	944	944
Reflns collected	9931	11866
Independent reflns	3758	7317
Completeness	98.1 %	99.6%
R(int)	0.0877	0.0245
Refinement method	Full-matrix least-squares on F^2	Full-matrix least-squares on F^2
Data / restraints / parameters	3758 / 0 / 307	7317/1/615
GOF on F^2	0.952	1.024
$^aR_1[I>2\sigma(I)]$, wR_2	0.0645, 0.1130	0.0427,0.0928
R_1[all data], wR_2	0.1283, 0.1397	0.0547,0.1010

$^aR_1=\Sigma||F_o| - |F_c||/\Sigma|F_o|$, $wR_2=[\Sigma[w(F_o^2 - F_c^2)^2]/\Sigma w(F_o^2)^2]^{1/2}$

Table 2

Compounds	T_d[a] (°C)	λAbs[b,c] (nm)	λ_{max}PL[b,c] (nm)	HOMO/LUMO[exp] (E_g^{opt})[d](eV)	HOMO/LUMO[cal] (E_g^{opt})[e](eV)	Φ[f]
BCzBTZ	347	344/352	448/447	-5.71/-2.73(2.98)	-5.31/-1.60	0.52
CzBBTZ	340	294,342/296,352	452/448	-5.72/-2.65(3.07)	-5.37/-1.85	0.33

a)Loss of 5 wt%; b) UV-vis absorption and PL spectra in CH_2Cl_2; c) UV-vis absorption and PL spectra in neat film; d) Obtained from CV and the onset of UV-vis absorption spectra in film; e) Obtained from DFT calculations using B3LYP/6-31G(d,p); f) Measured by the integrating sphere system with neat film.

Table 3

Emitter	CIE	L_{max}	CE_{max}	EQE_{max}	Devices @100 cd m^{-2}		Devices @1000 cd m^{-2}	
	(x,y)	cd/m^2	cd/A	%	η_c(cd/A)	η_e (%)	η_c(cd/A)	η_e (%)
BCzBTZ	(0.15, 0.08)	8295	1.39	1.40	1.37	1.39	1.39	1.39
CzBBTZ	(0.15, 0.10)	812	0.52	0.20	0.31	0.11	--	--

Figures and Scheme

Figure 1 (a) the molecule structure; (b) the stacking structure with all atoms along the Axis b for BCzBTZ and the Axis c for CzBBTZ; (c) the stacking structure omitting hydrogen atoms along the Axis b for BCzBTZ and the Axis a for CzBBTZ;(d) The spatial distribution of the two adjacent molecules in crystal package.

Figure 2 (a) TGA profiles of BCzBTZ and CzBBTZ ; (b) Cyclic voltammetry curves of BCzBTZ and CzBBTZ.

Figure 3 a) UV-vis absorption of BCzBTZ and CzBBTZ in DCM solution and thin film; b) PL spectra of BCzBTZ and CzBBTZ in DCM solution and thin film; c) PL spectra of BCzBTZ in different solvents; d) PL spectra of CzBBTZ in different solvents.

Figure 4 Calculated spatial distributions of HOMOs and LUMOs of TPABTZ, BCzBTZ and CzBBTZ.

Figure 5 HOMO–LUMO levels of the used materials.

Figure 6 (a) J–V_B characteristics; (b) V-L curves; (c) current efficiency; (d) EL spectra of BCzBTZ and CzBBTZ based OLEDs.

Scheme 1 Synthesis and structures of target compounds.

Figure 1

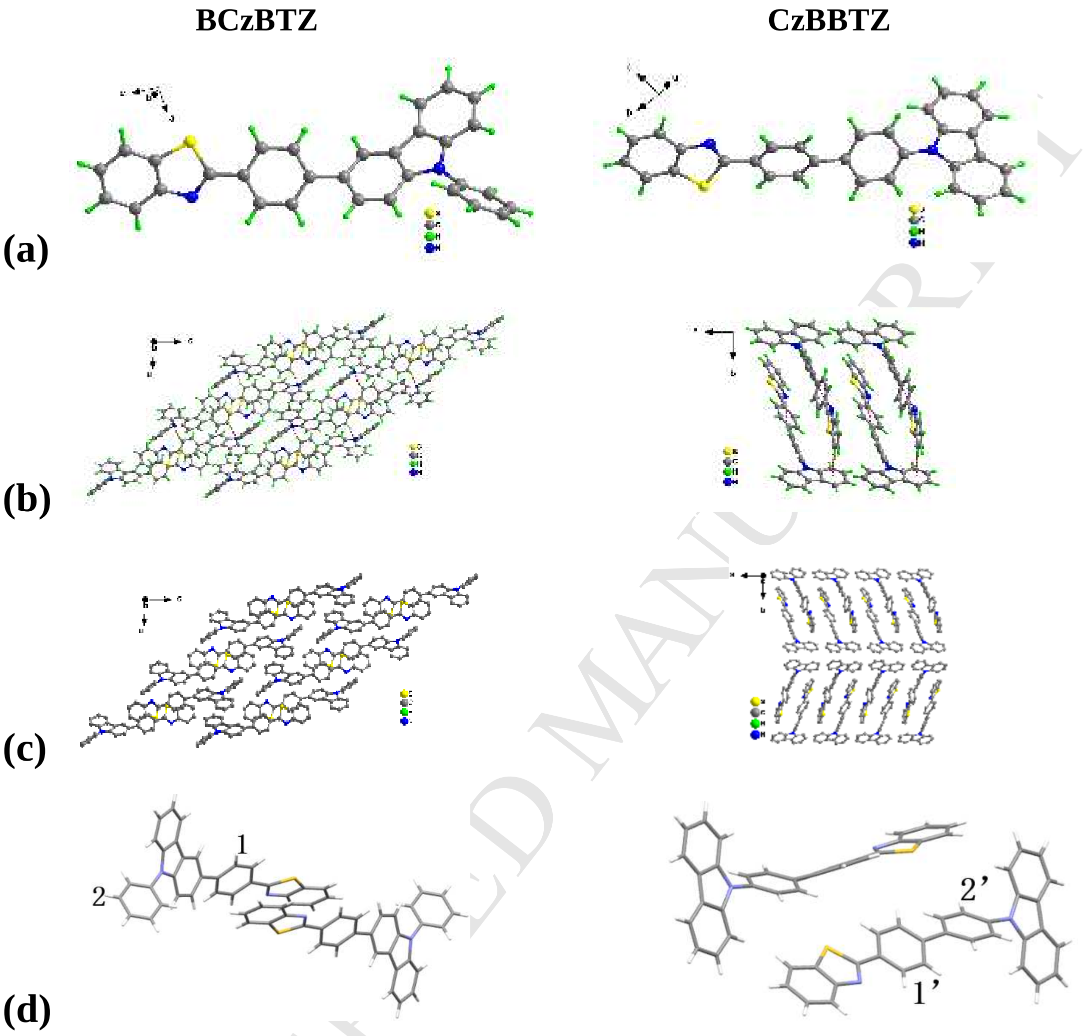

Figure 2

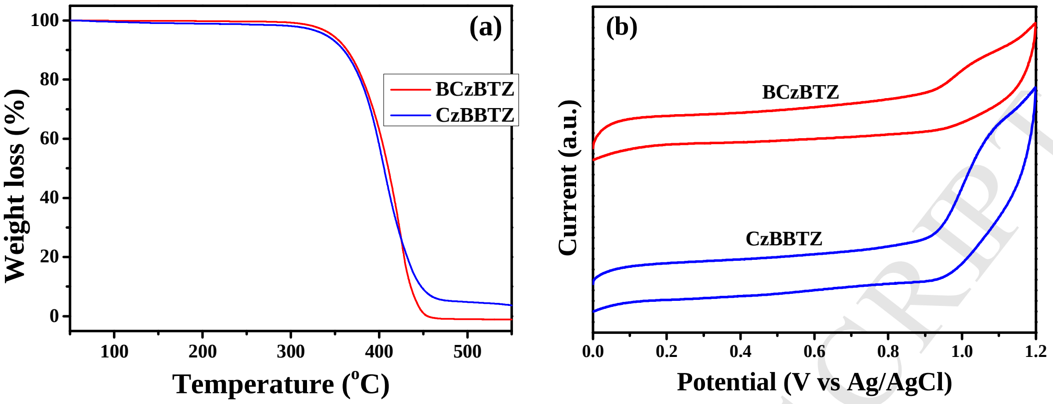

Figure 3

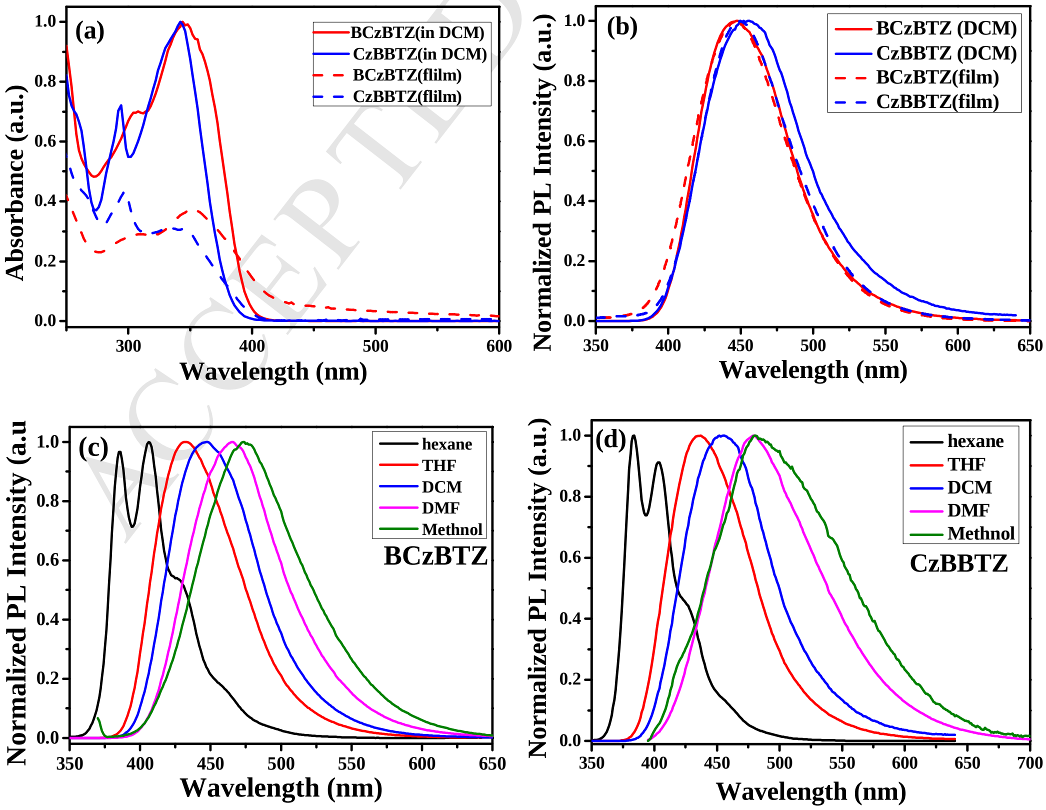

Figure 4

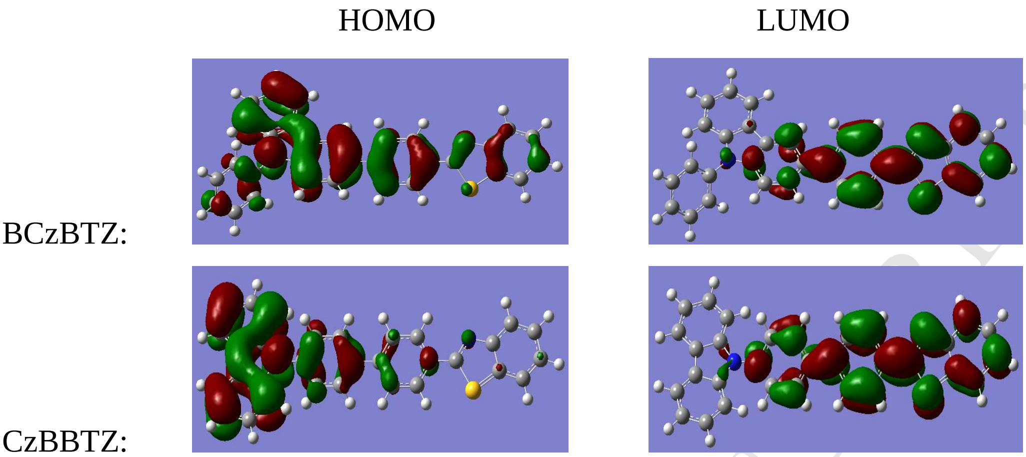

Figure 5

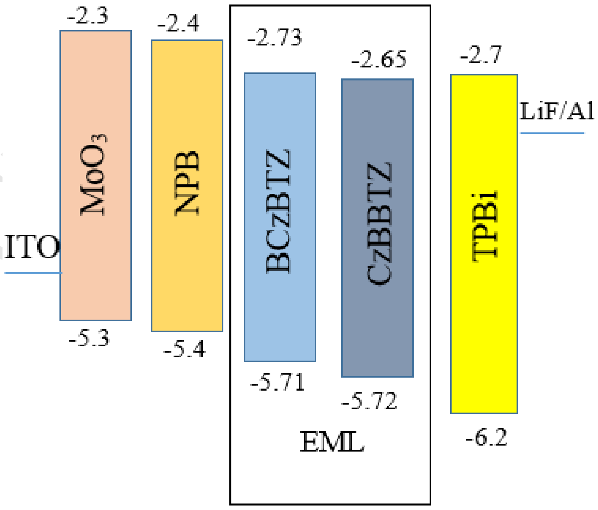

Figure 6

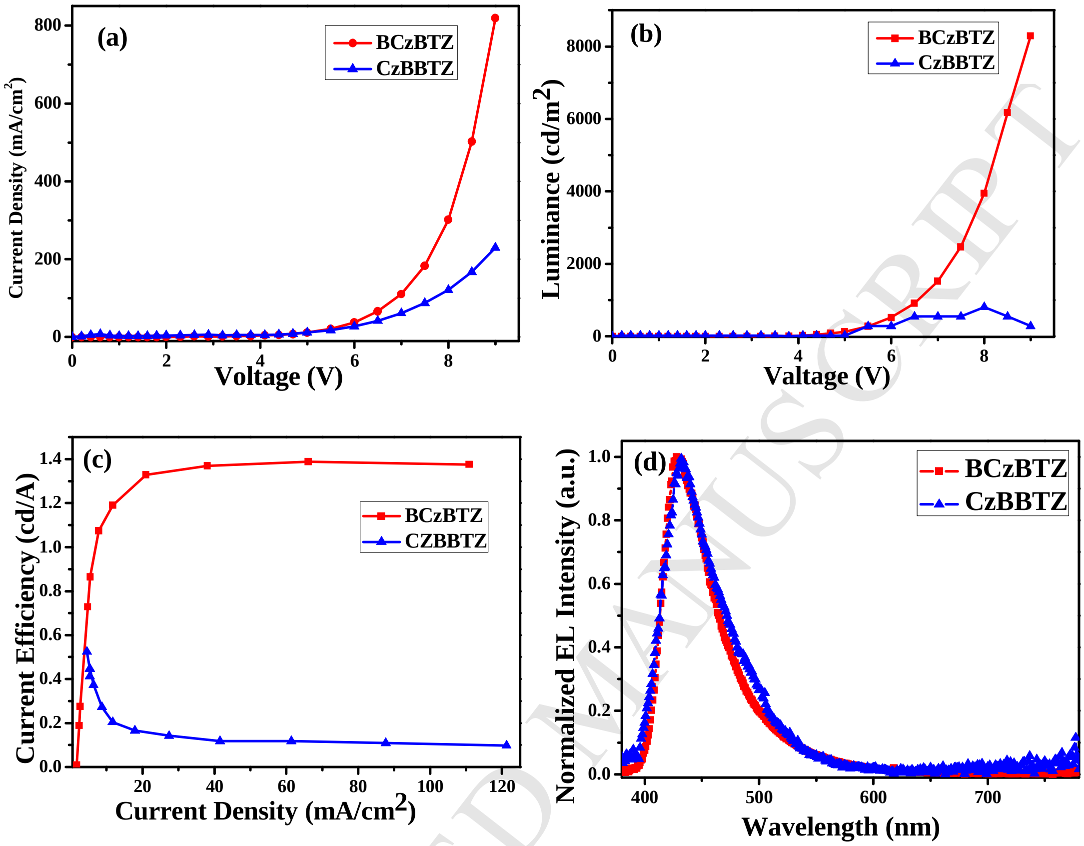
(a)
BCzBTZ
CzBBTZ
Current Density (mA/cm²)
800
600
400
200
0
0
2
4
6
8
Voltage (V)
(b)
BCzBTZ
CzBBTZ
Luminance (cd/m²)
8000
6000
4000
2000
0
0
2
4
6
8
Valtage (V)
(c)
BCzBTZ
CZBBTZ
Current Efficiency (cd/A)
1.4
1.2
1.0
0.8
0.6
0.4
0.2
0.0
20
40
60
80
100
120
Current Density (mA/cm²)
(d)
BCzBTZ
CzBBTZ
Normalized EL Intensity (a.u.)
1.0
0.8
0.6
0.4
0.2
0.0
400
500
600
700
Wavelength (nm)

Scheme 1

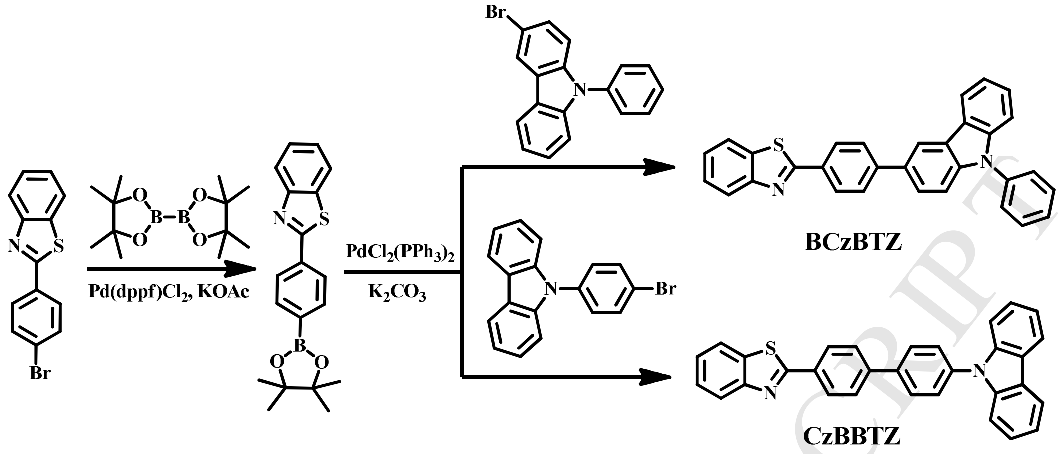

Highlights

- Two novel benzothiazole derivatives were synthesized and characterized.
- The differences of their performance were discussed according to the crystal structure.
- The device based on BCzBTZ as emitter shows deep-blue emission with the CIE(x, y) of (0.15, 0.08).